Petroleum Science 19 (2022) 2387–2398

Contents lists available at ScienceDirect

Petroleum Science

journal homepage: www.keaipublishing.com/en/journals/petroleum-science

Original Paper

Reliability analysis of large-diameter high-grade-steel natural gas pipelines under fault action

Xiao-Ting Gu [a, b], Xue-Rui Zang [c, *], Zhen-Yong Zhang [d], Peng Yang [e], Wen-Zhen Miao [f], Ping Cao [g], Bin Zhao [h]

[a] School of Petroleum Engineering, Yangtze University, Wuhan, 430100, Hubei, China
[b] Key Laboratory of Drilling and Production Engineering for Oil and Gas, Wuhan, 430100, Hubei, China
[c] College of Pipeline and Civil Engineering, China University of Petroleum (East China), Qingdao, 266580, Shandong, China
[d] China Petroleum Pipeline Engineering Corporation, Langfang, 065000, Hebei, China
[e] China Petroleum Pipeline Engineering Co., Ltd., Langfang, 065000, Hebei, China
[f] Sinopec Zhongyuan Petroleum Engineering Design Co., Ltd., Zhengzhou, 450000, Henan, China
[g] Sinopec Jianghan Petroleum Engineering Design Co., Ltd., Wuhan, 430223, Hubei, China
[h] College of Geophysics and Oil Resources, Yangtze University, Wuhan, 430100, Hubei, China

ARTICLE INFO

Article history:
Received 27 September 2020
Accepted 1 September 2021
Available online 24 June 2022

Edited by Xiu-Qiu Peng

Keywords:
Trench parameters
Natural gas pipeline
Fault
Soil-pipeline interaction
Soil spring stiffness

ABSTRACT

There are a lot of researches on qualitative aseismatic measures for buried gas pipeline crossing movable faults. But a few of them are quantitative, especially in the size and shape of the trench. The paper first established the finite element model of the strain of buried pipeline crossing a fault which effected by the size and shape of the trench. And it obtained new soil spring stiffness which considered different buried depth, bottom width of trench, trench slope and elastic modulus of soil. The mechanical analysis model of pipeline is established, and the limit state equation of pipeline is fitted. The reliability and sensitivity of the natural gas pipeline under fault action are analysed by a Monte Carlo method, and the error and accuracy are verified. When the pipeline is under tension, the sensitivity from large to small is buried depth, sand friction angle, pipe diameter, pipeline displacement, trench bottom width, trench depth, clay cohesion, trench slope and clay friction angle; when the pipeline is under pressure, the trench depth and clay cohesion have great influence. The findings of this study provide a reference for pipeline design and safety evaluation under fault action.

1. Introduction

High steel grade is the development trend of natural gas pipeline, considering the social conditions and economy, the gas pipeline inevitably needs to cross fault area, which leads to the frequent occurrence of earthquake disasters during the pipeline operation, and causes serious damage to the safety of the pipeline. Since 1975, scholars home and abroad (Newmark and Hall, 1975; Kennedy et al., 1977; Wang and Yeh, 1985; Wang and Wang, 1995; Karamitros et al., 2007, 2011; Liu et al., 2008; Trifonov and Cherniy, 2010; Joshi et al., 2011; Jalali et al., 2016; Cheng et al., 2019) have conducted a large number of analysis on the stress of the pipeline across the fault.

In recent years, with the increasing attention to the seismic vulnerability of pipelines, scholars home and abroad have done a lot of research on pipeline deformation and pipeline reliability. Gu and Zhang (2009) conducted a more in-depth study on the seismic design method of buried pipelines crossing active faults; established a soil spring stiffness calculation method which considers the laying parameters of pipe trench, and on this basis, the mechanical calculation model of pipeline crossing active fault was established. Vasileios et al. (2014) transformed seismic data to structural analysis by using the vector strength measurement method of fault displacement, obtained strain risk curves by combining the numerical simulation results and hazard analysis. Liu et al. (2017) have proposed a calculation method of design strain of X80 pipelines subjected to the action of three-dimensional oblique reverse faults. Li et al. (2019) analysed the influence of different sensitivity factors on the strain response of submarine pipeline crossing strike slip fault by finite element method. Li and

* Corresponding author.
E-mail address: 15192775783@163.com (X.-R. Zang).

https://doi.org/10.1016/j.petsci.2022.06.017

List of abbreviations

BP	Error Back Proragation
ASCE	The American Society of Civil Engineers
SLS	Serviceabilty Limit State
ULS	Ultimate Limit States
LLS	Leak Limit State
ALS	Accidental Limit States
FLS	Fatigue Limit States

List of symbols

ε_0	initial strain
σ_s	yield stress, MPa
E	modulus of elasticity, MPa
δ_p	vertical displacement, m
β	the pipeline and the fault, degree
$[\varepsilon]$	allowable strain
ε^{crit}	ultimate strain of the pipeline
F	safety factor
ε_t	tensile strain
s	maximum displacement of pipeline under the action of fault, m
h	buried depth of pipeline, m
D	pipe diameter, m
c	cohesive force of clay, MPa
t	thickness of cushion, m
b	widening allowance, m
m	sand friction angle, rad
n	friction angle of clay, rad
ε_c	compressive strain
μ	Poisson's ratio

He (2021) established a pipe-soil-fluid three-phase coupling model based on fluid-structure interaction (FSI) by using ADINA finite element software, and the influencing factors of mechanical response of buried gas pipelines across faults are studied. These pipeline deformation results mentioned above creates conditions for the calculation of pipeline reliability.

For Calculation of pipeline reliability, China National Petroleum Corporation (CNPC) has derived the domestic extreme limit state objective reliability calculation formula (Zhang et al., 2014), and proposed the risk acceptance criteria for China's oil and gas pipelines (Zhao et al., 2016). Tao and Sun (2015) adopted allowable length change and allowable compression strain in analysing the seismic reliability of buried pipelines crossing faults. Fan et al. (2016) proposed a direct calculation method of seismic pipeline reliability based on strain design combined with Q/SY-GJX-0136-2008 and a reliability design code. Zheng et al. (2020) established the design strain prediction model of Error Back Proragation (BP) double hidden layer neural network and carried out reliability calculation of X80 pipeline in strike slip fault area by combining Monte Carlo method.

In all the above studies, only Gu X T, Zhang H consider the influence of pipe trench parameters on pipeline-soil interaction.

(1) The buckling analysis is not comprehensive enough by employing the mixed model of tube element and bend element.
(2) The three-dimensional problem is simplified to a plane problem, which results in large calculation error and poor matching degree with the actual working condition.

Besides, there is no in-depth calculation of pipeline reliability. In fact, as one of the main control parameters, the pipe trench parameters directly affect the economy and effectiveness of the pipeline. Therefore, this paper uses PSI element method to establish a cross fault model considering the parameters of the pipe trench, obtains the strain regression formula, and carries out the reliability analysis of the pipeline. The research results are significant in the design and safety evaluation of pipelines under fault actions, it also provides theoretical support for the reliability industry standards of seismic pipeline.

2. Three-dimensional pipe-soil contact analysis model of natural gas pipeline under fault action

In this study, ABAQUS software is adopted to build the 3D numerical model (Liu et al., 2020; Wei et al., 2021; Zhang et al., 2021). Because the pipeline subjected to the fault reflects double nonlinear problems of material nonlinearity and geometric nonlinearity, to obtain the soil spring stiffness more accurately, a shell element model is used for modelling the pipe to simulate the actual situation more precisely.

(1) Ramberg-Osgood constitutive model

The Ramberg-Osgood equation is a theoretical model in solid mechanics that describes the stress-strain relationship (stress-strain curve) of a material near its yield point (Fig. 1). It's a better representation of real material. The constitutive relationship is in the form of:

$$\varepsilon_{ture} = \frac{\sigma_{ture}}{E}\left[1 + \frac{\alpha}{1+n}\left(\frac{\sigma_{ture}}{\sigma_s}\right)^n\right] \quad (1)$$

Where ε_0 is initial strain, $\varepsilon_0 = \sigma_s/E$; σ_s is yield stress; E is modulus of elasticity; α is Hardening coefficient, $\alpha = 22.54$; n is Power hardening index, $n = 22.98$.

(2) Parameters of material properties

The X80 pipeline of the Second West-East Gas Pipeline is selected, the pipeline uses a Ramberg-Osgood constitutive model, and its mechanical parameters are listed in Table 1.

(3) Parameters of soil mechanics

The soil uses a Mohr Coulomb constitutive model, and its parameters (Yu et al., 2010; Wang et al., 2011; Li et al., 2013) are presented in Table 2.

2.1. Soil spring stiffness model effected by trench parameters

2.1.1. Three-dimensional contact solid model

At present, the selection of three-dimensional soil-spring stiffness and limit load mostly use guidelines for the seismic design of oil and gas pipeline systems from The American Society of Civil Engineers (ASCE). The soil spring model in ASCE can not reflect the situation that mechanical properties of original soil and back fill soil are different, and the influence of trench, because it based on mechanical properties of soil which in the scope of infinity outside pipeline are some.

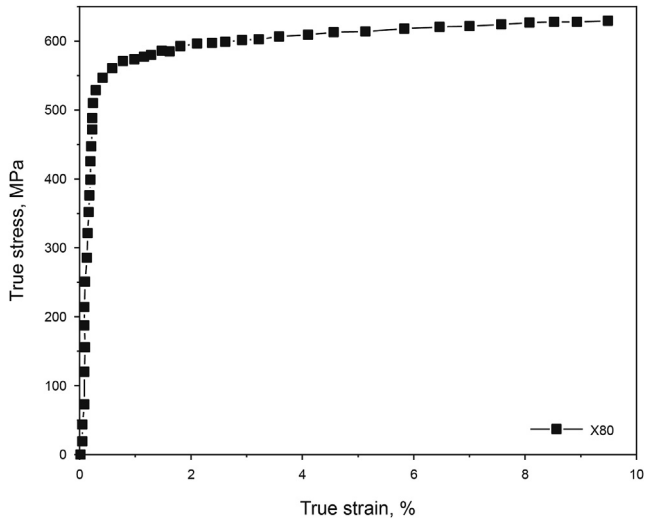

Fig. 1. True stress versus strain curve for X80 pipe.

The paper first established the finite element model of the strain of buried pipeline crossing a fault which effected by the size and shape of the trench. And it obtained new soil spring stiffness which considered different buried depth, bottom width of trench, trench slope and elastic modulus of soil.

ABAQUS was used to establish a 3D finite element model, considering the dual nonlinear problems of material nonlinearity and geometric nonlinearity, the pipeline model adopts a four-node curved shell reduced integral element (S4R) for finite membrane strain. The soil model uses an eight-node linear hexahedron element (C3D8). The master-slave contact algorithm is adopted for the pipe-soil contact setting: the master surface is the external surface of the pipe, whereas the slave surface is the soil surface in contact with the pipe. The tangential action defines the friction coefficient between the pipe and soil using a penalty function. The normal action is set to 'hard contact'. The 3D finite element model with pipe trench and mesh generation are illustrated in Fig. 2.

2.1.2. Load boundary conditions

Applying the method of solving the load by positioning displacement and obtaining the soil resistance in all directions by applying displacement. As shown in Fig. 3, the limit load and limit load deformation of 3 point can be got under apply concentrated force on 1 point in the outer surface of the pipeline by using the finite element method. The ratio of the limit load to limit load deformation of 3 point is the vertical upward soil spring stiffness. The vertical upward and horizontal soil spring stiffness can be got in the same method.

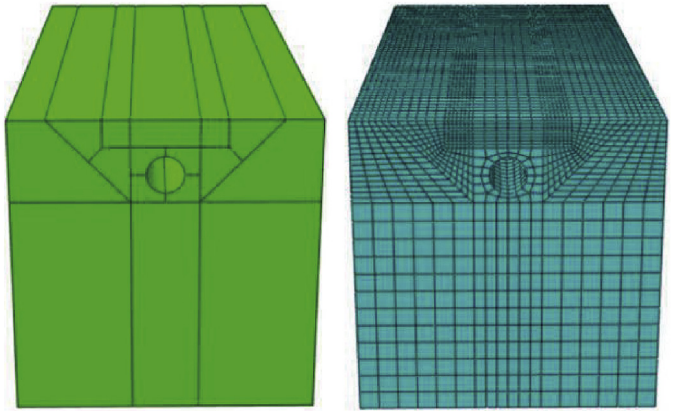

Fig. 2. Three-dimensional finite element model with pipe trench.

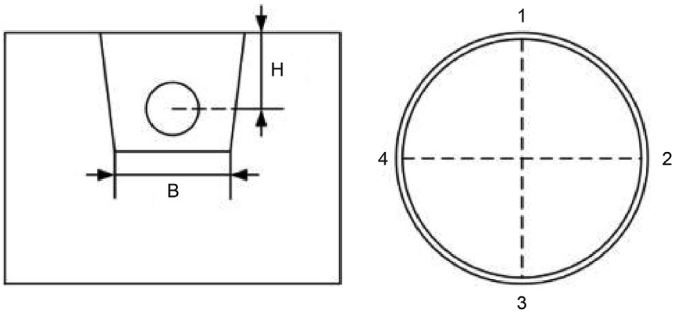

Fig. 3. Trench model.

The boundary conditions are as follows: the upper surface is free, the lower surface constrains all degrees of freedom of displacement, both ends of the pipe and other surfaces of the soil constrain the normal degrees of freedom.

There are two ways of determining the load-displacement curve: provide the load to solve the displacement or provide the displacement to solve the load. To avoid convergence problems caused by the decrease in stiffness (even to zero) when reaching the limit condition, this model applies the method of solving the load by positioning displacement and obtaining the soil resistance in all directions by applying displacement.

2.2. Grid independence verification and model verification

2.2.1. Grid independence

In order to obtain a reasonable grid to ensure the calculation accuracy and the appropriate amount of calculation, this paper

Table 1
Mechanical parameters of X80 pipeline of Second West-East Gas Pipeline.

Pipe diameter D, mm	Wall thickness Δ, mm	Buried depth H, m	Young's modulus E, MPa	Poisson's ratio μ	Minimum yield strength $\sigma_{s\,min}$, MPa	Soil shear strength τ, MPa	Pipe soil friction coefficient
1219	22	1.80	210000	0.30	641	50	0.65

Table 2
Basic parameters of soil materials.

Soil type	Elastic modulus E, MPa	Poisson's ratio μ	Density ρ, kg/m^3	Friction angle θ, degree	Cohesive force C, kPa
Site soil	25	0.45	1800	20	50
Sandy soil	11.90	0.30	1700	35	1

Table 3
Parameters of the mesh convergence test.

Mesh No.	Soil grid	Pipe grid	Total number of grids	Calculate time loss t, s	Maximum stress value σ_{max}, MPa	Pipe displacement S, m
No.1	2288	800	3080	33	399.40	1.60
No.2	2288	1200	3480	56	470.20	1.62
No.3	4576	1200	5776	1003	508.70	1.68
No.4	4576	1600	6176	1200	529.30	1.77
No.5	9152	3200	12352	4790	538.40	1.75

Table 4
Model validation results.

Resistance direction	Model calculation	ASCE theoretical calculation	Relative error
Axial	35	36.02	2.83%
Horizontal	428	453.90	5.71%
Vertical upward	203.20	206.50	1.60%
Vertical downward	1326	1197	9.70%

Table 5
Partial running results of 3D model.

Axial direction Y, KN	Axial direction X, m	Vertical upward Y, KN	Vertical upward X, m	Vertical downward Y, KN	Vertical downward X, m	Horizontal direction Y, KN	Horizontal direction X, m
−490.32	-3.81×10^{-3}	14156.33	1.50×10^{-2}	−4075950	12.19×10^{-2}	647246	8.44×10^{-2}
−550.38	-3.81×10^{-3}	19493.15	1.50×10^{-2}	−4237792	12.19×10^{-2}	750966	8.44×10^{-2}
−611.37	-3.81×10^{-3}	26458.48	1.50×10^{-2}	−4399633	12.19×10^{-2}	905702	8.44×10^{-2}
−673.27	-3.81×10^{-3}	34785.29	1.50×10^{-2}	−4561474	12.19×10^{-2}	1091797	8.44×10^{-2}
−736.09	-3.81×10^{-3}	44220.01	1.50×10^{-2}	−4723316	12.19×10^{-2}	1290074	8.44×10^{-2}
−799.83	-3.81×10^{-3}	54743.31	1.50×10^{-2}	−4885157	12.19×10^{-2}	1481841	8.44×10^{-2}
−864.49	-3.81×10^{-3}	66855.46	1.50×10^{-2}	−5046998	12.19×10^{-2}	1648974	8.44×10^{-2}
−77.40	-3.81×10^{-3}	20171.76	1.50×10^{-2}	−218540	12.19×10^{-2}	173373	8.44×10^{-2}
−185.81	-3.81×10^{-3}	20713.30	1.50×10^{-2}	−703184	12.19×10^{-2}	314955	8.44×10^{-2}
−326.38	-3.81×10^{-3}	22926.98	1.50×10^{-2}	−1678308	12.19×10^{-2}	549631	8.44×10^{-2}
−407.79	-3.81×10^{-3}	24041.64	1.50×10^{-2}	−2385242	12.19×10^{-2}	662333	8.44×10^{-2}
−511.83	-3.81×10^{-3}	25327.58	1.50×10^{-2}	−3390705	12.19×10^{-2}	780316	8.44×10^{-2}
−706.39	-3.81×10^{-3}	27473.98	1.50×10^{-2}	−5331927	12.19×10^{-2}	1080379	8.44×10^{-2}

conducts grid independence verification. Taking Mises stress and the maximum displacement of the pipeline as the selection criteria for the optimized grid, five grid types are established, as shown in Table 3. The grid types are all hexahedral structural grids.

Table 3 shows that for grid No. 1–2, the Mises stress caused by soil displacement is between 430 and 500 MPa, while the Mises stress of grid No. 3–5 is concentrated between 520 and 540 MPa. The results of the two parts are quite different. By sequentially densifying the grids, the pipe-soil displacements of the No. 4 and No. 5 grids are basically the same. When the number of grids reaches 6176, the error between adjacent grid densities is within 2%, indicating that the grid density basically has no effect on the simulation results. However, the calculation of grid No. 5 greatly exceeds other grid sizes. Therefore, the model adopts the 4th grid accuracy. The model adopts a hexahedral structural grid as a whole, a pipe with 4 nodes, a curved thin shell reduced integral element (S4R), and a finite membrane strain; the mesh element type of the soil is an 8-node linear hexahedral element (C3D8R). When this type of grid is deformed, it has little effect on the analysis accuracy and can accurately solve the displacement. In order to improve the calculation accuracy and save the calculation resources, the mesh of the pipe-soil contact area is refined. The total number of grids is 6176, among which the number of refined grids is 3185.

2.2.2. Model verification

Since the test and model of pipe trench parameters are not considered at present, to verify the soil-spring stiffness calculation model considering the trench parameters, the results of a trenchless model under the same working conditions are compared with ASCE standards (1984). The calculation results of the soil resistance value reaching the maximum yield displacement for the first time in all directions are compared with the unit length calculated from the ASCE standards. The validation results are shown in Table 4.

It can be seen from Table 4 that the relative error is within 10%, and the model is feasible.

3. Numerical model of natural gas pipeline crossing faults

PSI element method is an effective method to analyse the interaction between pipe and soil. In this chapter, when establishing the cross-fault model, PSI element method is selected to establish the model for extracting the strain value of each pipe section more conveniently. The theoretical model of PSI element method is shown in the Fig. 4 below.

3.1. Finite element model

(1) The pipeline is modeled by shell element. The shell element can be easily used in the model of thin-walled structures, and accurate results can be obtained. At the same time, it avoids the complexity and scale of using solid elements to build such structures.
(2) A PSI element is used to simulate the soil-pipe interaction. The stiffness of the soil-spring of the PSI element can be

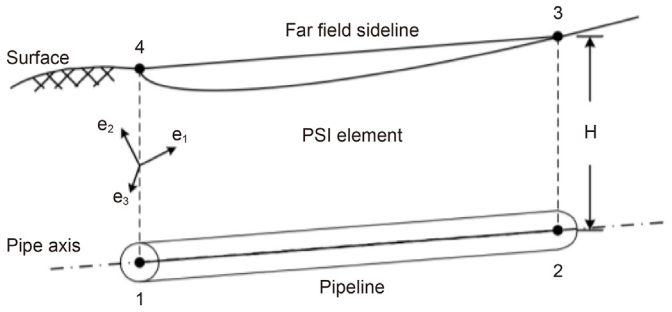

Fig. 4. PSI element method.

Table 6
Boundary conditions.

Fault parameter	Δ*x*, m	Δ*y*, m	Δ*z*, m
Numerical value	1.36	−1.60	−3.80

obtained by 2.1 Soil spring stiffness model effected by trench parameters. Some of the data are presented in Table 5.

(3) By introducing equivalent boundary conditions, the left and right ends of the model are constrained by *x*-direction displacement, and the symmetrical plane is constrained by symmetry.

(4) Based on the actual data of the Second West-East Gas Pipeline, the displacement load is applied to the PSI element, and the internal pressure load is applied to the elbow unit. When the pipeline crosses a normal fault and reverse fault with vertical displacement δ_p, the horizontal component $\Delta x = \delta_p \cos\varphi \sin\beta + \delta_s \cos\beta$, horizontal lateral component $\Delta y = \delta_p \cos\varphi \cos\beta - \delta_s \sin\beta$, and vertical component $\Delta z = \delta_p \sin\varphi$ along the pipeline.

The parameter δ_p becomes a positive value for a normal fault and a negative value for a reverse fault. Additionally, δ_s becomes a positive value for a right-hand strike-slip fault and a negative value for a left-hand strike-slip fault. The intersection angle β between the pipeline and the fault is defined as the angle between the ground movement direction on the right side of the fault and the right direction of the pipeline axis. The specific parameters are shown in Table 6.

(5) The steel grade of the pipe is X80, and the Ramberg-Osgood constitutive model is applied. The steel pipe parameters are determined by the fitting of the real stress-strain curve measured from the tensile test.

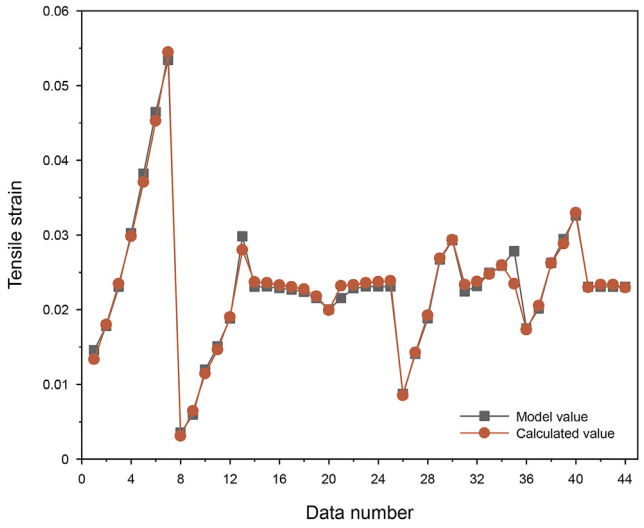

Fig. 6. Fitting results of tensile strain.

Based on the method above, the finite element model of the crossing fault is established with a total length of 2200 m, which is the reverse strike-slip fault located in the middle of the model. The fault area is 100 m to the left and right of the fault, as shown in Fig. 5.

4. Seismic limit state equation of natural gas pipeline based on strain

The seismic limit state equation of natural gas pipeline based on strain is given in Eq. (2).

$$\varepsilon - [\varepsilon] = 0 \tag{2}$$

4.1. Allowable strain

Following Q/SY 1603–2013 standards of CNPC, the allowable strain is expressed as the ultimate strain divided by the safety factor:

$$[\varepsilon] = \frac{\varepsilon^{\text{crit}}}{F} \tag{3}$$

Where $[\varepsilon]$ is the allowable strain; $\varepsilon^{\text{crit}}$ is the ultimate strain of the pipeline; F is the safety factor.

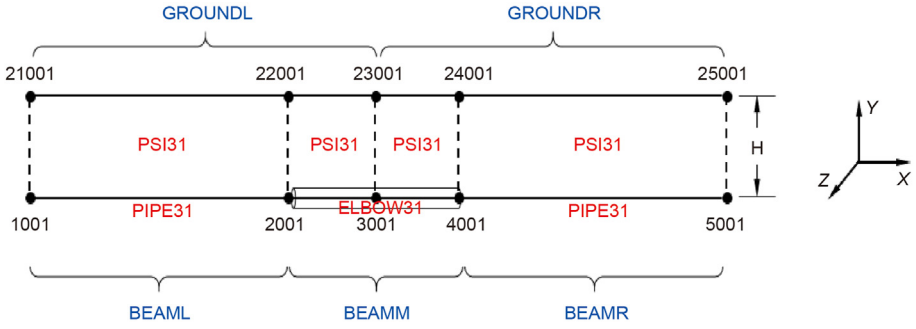

Fig. 5. Pipeline model of crossing fault.

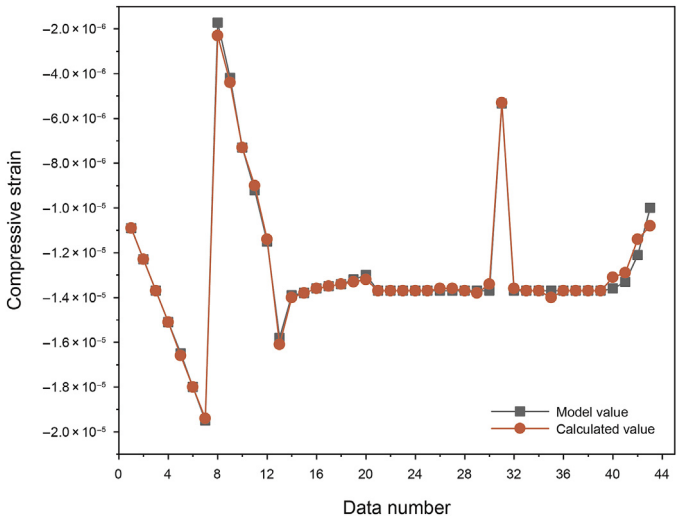

Fig. 7. Fitting results of compressive strain.

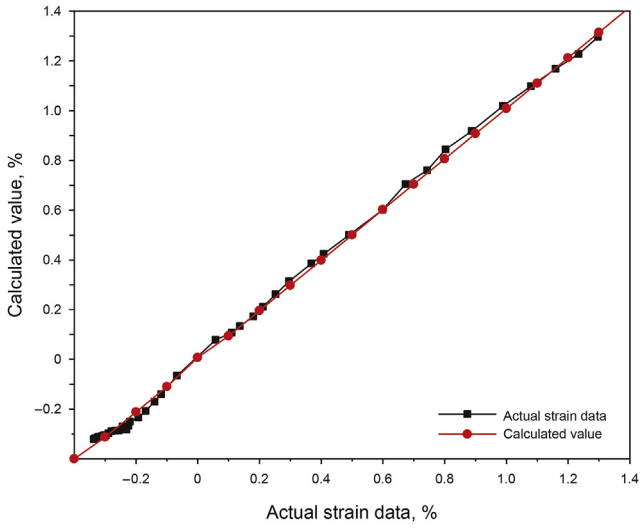

Fig. 8. Relationship between calculation results and field data.

4.2. Pipeline strain

From the established mechanical calculation model of pipeline crossing through active faults, the strain law of natural gas pipeline under different working conditions is analysed. Statistical analysis of the pipeline strain under different working conditions is carried out to obtain the strain regression formula of the natural gas pipeline under the action of faults.

4.2.1. Tensile strain design formula

Based on the calculation results of the pipe-soil model with trench under the action of fault, this section applies the global optimization algorithm of 1stOpt software to modify the strain regression formula without pipe trench (Liu et al., 2014). The fitting data of the tensile strain is as follows:

$$\varepsilon_t = -0.0602sh^{2.2793}\left(\frac{D}{s}\right)^{1.1093}\left(c^{0.8449}+49.3436\right)\left(t^{0.0119}-0.9393\right)\left(b^{3.954}-623.413\right)\left[(\pi-m)^{0.2597}-0.1224(\pi-m)^{1.1016}-0.9228\right]\left(-0.0727\sin^{3.5467}(n)-0.1719\sin^{-0.0319}(n)+0.2929\right)\left(1.1865\sin^{0.001}(u)+0.0023\sin^{23.1793}(u)-1.1606\right) \quad (4)$$

where ε_t is the tensile strain; s is the maximum displacement of pipeline under the action of fault; h is the buried depth of pipeline; D is the pipe diameter; c is the cohesive force of clay; t is the thickness of cushion; b is the widening allowance; m is sand friction angle; n is the friction angle of clay.

4.2.2. Compression strain design formula

The fitting data of the compressive strain is expressed as follows:

$$\varepsilon_c = 0.011sh^{0.9899}\left(\frac{D}{S}\right)^{1.0806}\left(c^{-4.0206}-0.000156\right)\times\left(t^{-1.8922}+63.9957\right)\left(b^{-0.0694}+0.0585\right)\left[(\pi-m)^{-1.9071}-4.4415(\pi-m)^{0.3129}+27.262\right]\left(2.778-3.4027\sin^{5.6952}(n)-0.1503\sin^{0.018}(n)\right)\left(0.3569+0.0432\sin^{-0.616}(u)-0.4029\sin^{-0.0779}(u)\right) \quad (5)$$

where ε_c is the compressive strain.

4.2.3. Analysis of fitting results

Fig. 6 and Fig. 7 respectively show the comparison between the calculated values of the fitting formula of tensile strain and compressive strain with the actual measured values. The judgment parameters of the fitting results are given in Table 7.

It can be seen from Table 7 that the standard deviation and residual sum of squares are close to zero, and the correlation coefficient and its square are close to one. The above parameters indicate that the fitting results are accurate, and the fitting formula has good accuracy and can be used for strain calculation of pipelines crossing faults.

Table 7
Judgment parameters of fitting results.

Comparison parameters	Mean square deviation	Sum of squares of residuals	Correlation coefficient	Square of correlation coefficient
Tensile strain	9.10×10^{-4}	3.65	99.50×10^{-2}	98.90×10^{-2}
Compressive strain	2.27	2.22	99.70×10^{-2}	99.50×10^{-2}

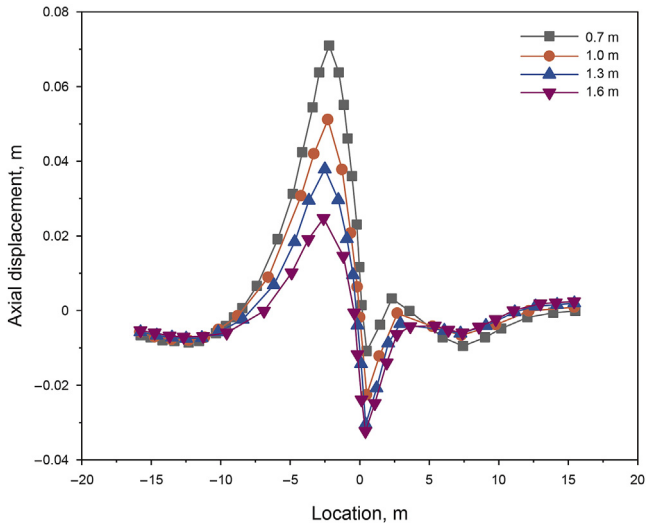

Fig. 9. Buried depth and axial displacement.

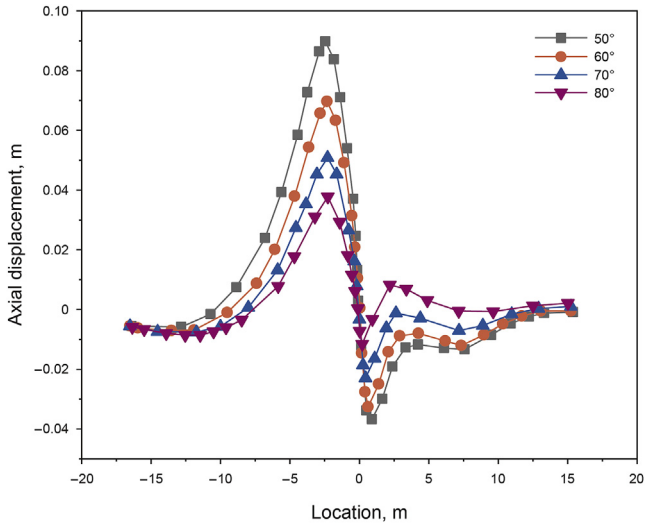

Fig. 11. Crossing angle and axial displacement.

4.2.4. Project case verification

To verify the accuracy of the three-way soil-spring fitting formula, according to the geological survey data of the Second West-East Gas Pipeline project, 40 groups of actual strain data (Cheng et al., 2016) are used for comparative analysis with the calculation results of the model, as presented in Fig. 8. The results indicate that the maximum strain error is 3.99%, and the minimum strain error is 0.01%. Through comparative analysis, the trend of fitting calculation results is the same as the actual working condition data. Therefore, it can be concluded that the fitting formula has a high fitting degree and certain accuracy.

5. Analysis of sensitive factors

(1) Buried depth

By controlling a single variant, the finite element models of 0.80 m, 1.20 m, 1.60 m and 2 m pipeline buried depth are established.

The results show that with the increase of the buried depth, the maximum axial displacement decreases and the maximum axial strain increases (Fig. 9 and Fig. 10). The axial displacement and the axial strain of the pipeline change greatly near the fault. The maximum tensile displacement of the pipe is located at −2.50 m with 0.08 m. The maximum compressive displacement of the pipe is located at 0.50 m with −0.04 m. The maximum tensile strain of the pipe is located at 1.20 m with a strain value of 2.02%. The maximum compressive strain of the pipe is located at −0.60 m with a strain value of −0.48%.

(2) Crossing angle

The finite element models of 50°, 60°, 70° and 80° pipeline crossing angles are established.

With the increase of pipeline crossing angle, the maximum values of axial displacement and axial compressive strain are obviously reduced, while the maximum values of axial tensile strain are almost unchanged (Fig. 11 and Fig. 12). These show that the compressive strain is more sensitive to the crossing angle and the larger crossing angle can effectively reduce the maximum values of axial displacement and axial compressive strain of

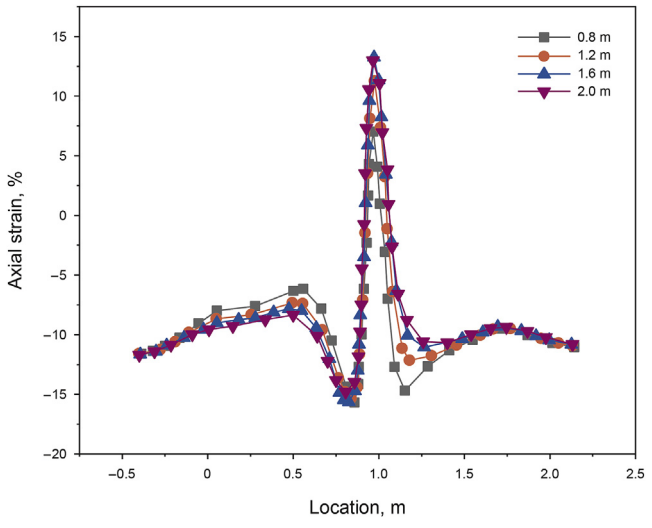

Fig. 10. Buried depth and axial strain.

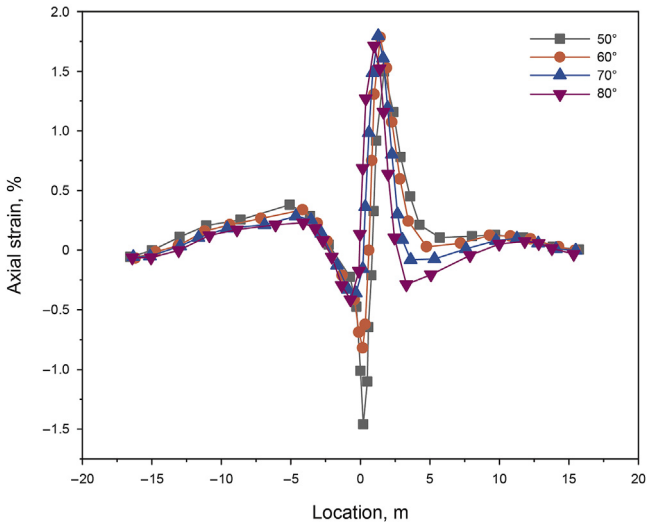

Fig. 12. Crossing angle and axial strain.

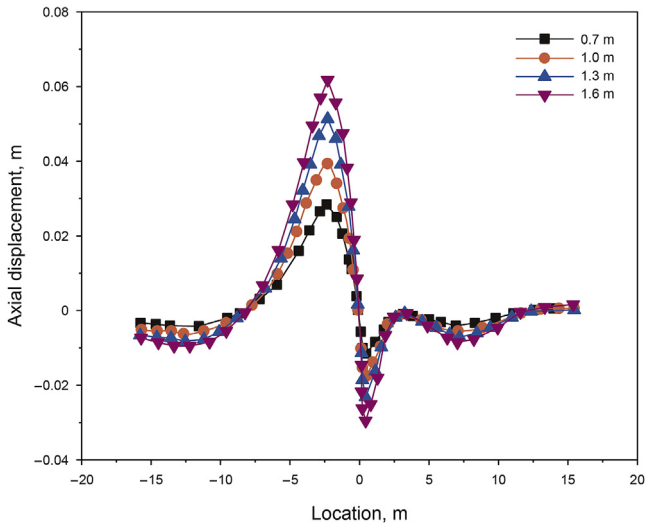

Fig. 13. Dislocation and axial displacement.

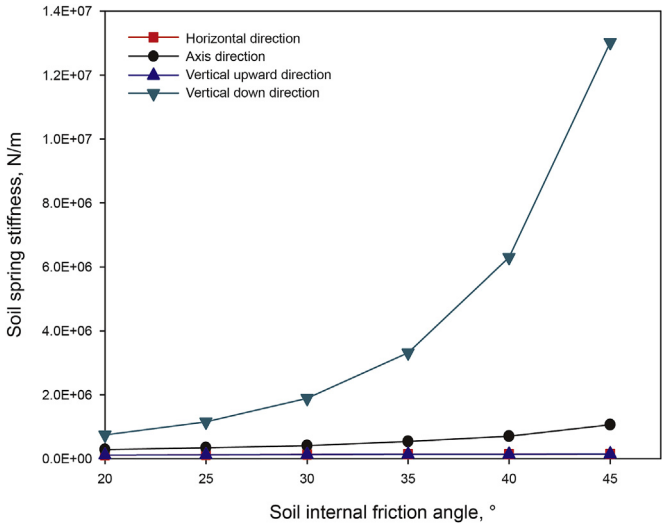

Fig. 15. Effect of internal friction angle of soil on soil spring.

pipeline.

(3) Dislocation

The finite element models of 0.70 m, 1 m, 1.30 m and 1.60 m faults with different dislocations are established.

From Fig. 13 and Fig. 14, The maximum value of axial displacement and axial strain increases with the increase of dislocation. This is due to the increasing shear force of soil around the pipeline, which increases the axial displacement and strain of the pipeline. The maximum tensile strain increases obviously with the increase of dislocation, while the maximum compressive strain is almost unchanged. This fully shows that under the influence of large dislocation, tensile deformation and failure are the main manifestations of the pipeline crossing fault.

(4) Soil internal friction angle

By controlling a single variable and changing the value of internal friction angle of soil, the influence on the stiffness of three-dimensional soil spring is obtained, as shown in Fig. 15.

It can be seen that the change of soil internal friction angle has a more significant impact on the vertical downward soil spring. When the soil internal friction angle reaches 35°, the vertical downward soil pressure per unit length increases exponentially.

(5) Soil pressure coefficient

Taking the K_0 value range of 0.50–1.30 involved in the design guidelines of the second west to east gas pipeline as an example, the influence of single variable K_0 value on soil spring in the direction of pipe axis is obtained as shown in Fig. 16.

It can be seen from the figure that with the increase of soil pressure coefficient, the pressure per unit length along the pipe axis increases, and the minimum and maximum values are 115872 N/m and 126422 N/m, respectively. Therefore, the soil pressure coefficient has little effect on the stiffness of soil spring along the pipe axis.

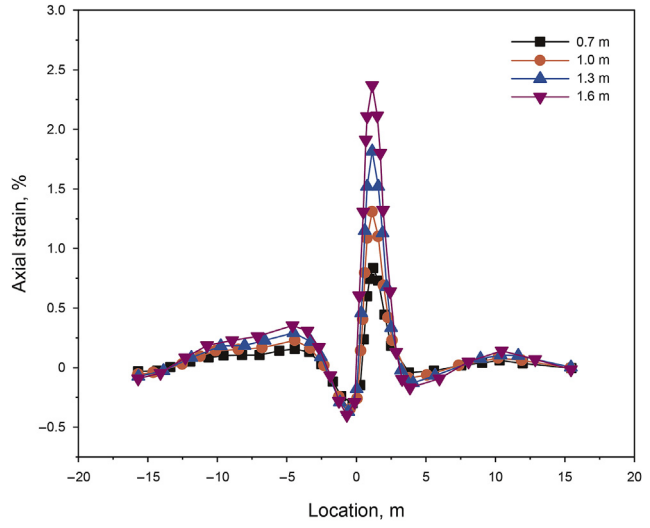

Fig. 14. Dislocation and axial strain.

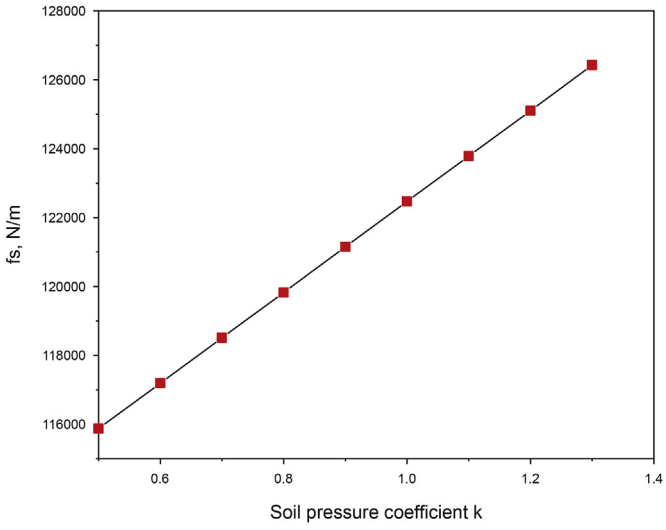

Fig. 16. Influence of soil pressure coefficient on soil spring in the direction of pipe axis.

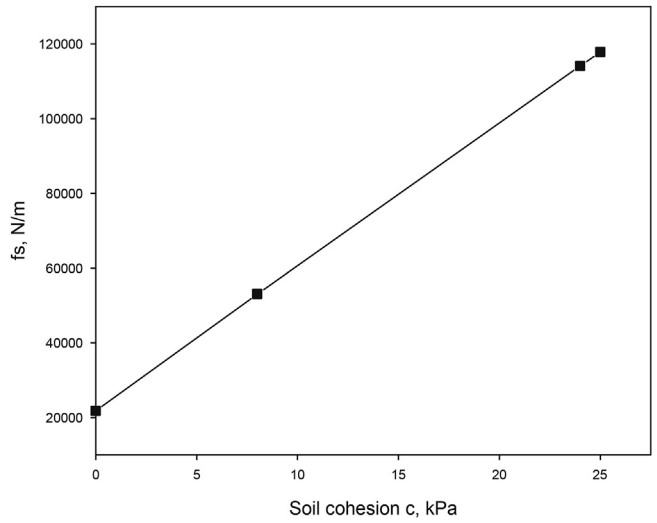

Fig. 17. Influence of soil cohesion on soil spring in the direction of pipe axis.

(6) Soil cohesion

Taking clay, loess, dense sand and sand as examples, the influence of single variable soil cohesion on soil spring along pipe axis is obtained, as shown in Fig. 17.

It can be seen from the figure that when the soil is sandy soil, the soil cohesion $c = 0$, and the minimum axial pressure per unit length of the pipeline is 21758 N/m; When the soil is clay, $c = 25$, the maximum axial pressure per unit length of the pipeline is 117850 N/m, which is 5.42 times of the former. Therefore, the influence of soil cohesion on the pipeline is more significant.

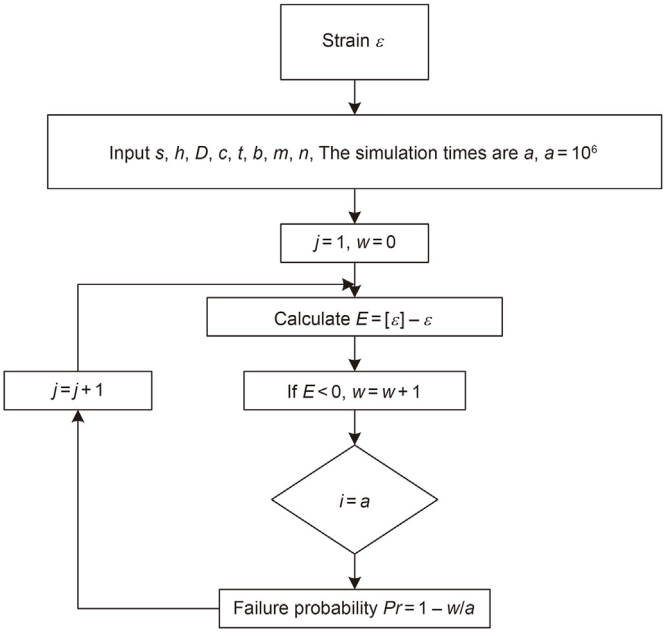

Fig. 18. The basic calculation flow of Monte Carlo.

6. Reliability analysis of natural gas pipeline under the action of fault

6.1. Monte Carlo method

In this paper, Monte Carlo method (Chen et al., 2013; Li and Shen, 2015) is used to analyse the reliability of natural gas pipeline under fault action. This is a sampling method to solve the reliability problem by sampling samples from the same function through a large number of random simulations and statistical tests. According to Bernoulli limit theorem, let x_1, x_2, L, x_n be n independent random variables. If they come from the same function, have the same distribution, and have the same finite-time average μ and variance σ^2, then for any $\varepsilon > 0$:

$$\lim_{n\to\infty} P\left(\left|\frac{1}{n}\sum_{i=1}^{n}(X_i - \mu)\right| \geq \varepsilon\right) = 0 \tag{6}$$

If the probability of occurrence of random event A is set as P(A), the occurrence frequency m and frequency $W(A) = m/n$ are obtained after n independent tests, then for any $\varepsilon > 0$, there is:

$$\lim_{n\to\infty} P\left(\left|\frac{m}{n} - P(A)\right| < \varepsilon\right) = 0 \tag{7}$$

From formulas (6) and (7), it can be obtained that when n is large enough, $\frac{1}{n}\sum_{i=1}^{n}x_i$ converges to μ according to probability, while frequency m/n converges to P (A) with probability 1.

The realization of Monte Carlo method needs the help of computer software. This paper uses MATLAB software. By inputting s (displacement), h (buried depth), D (pipe diameter), c (clay cohesion), t (pipe trench depth), b (pipe trench bottom width), m (sand friction angle), n (clay friction angle), and setting the number of each cycle to 106, the accuracy of the calculation results is ensured, and finally the reliability of the pipeline is obtain. The basic calculation flow of Monte Carlo method is shown in Fig. 18.

6.2. Target reliability

Target reliability (Zhang and Feng, 2013; Zhang et al., 2016; Wisianto and Kodivat, 2003; Hassanien et al., 2016; Yu et al., 2018) is an index to determine whether the pipeline is safe or not. Many international standards have given the calculation method of target reliability of oil and gas pipeline, such as: ISO 16708-2006, CSA Z662-2011, GB/T 29167-2012 and DNV-OS-F101. The details are shown in Table 8.

In this paper, the most widely used API 579 "Fitness-For-Service" is used as the target reliability to evaluate the safety performance of pipeline. According to API 579 standards, the first category of areas corresponds to low risk, the second category corresponds to medium risk, and the third and fourth category correspond to high risk.

According to statistics, each parameter conforms to the normal distribution. Refer to the statistical results of pressure fluctuations in the gas pipelines of Sichuan-Foshan Line and Henan Zhong'an County, the transmission pressure satisfies the normal distribution, and the coefficient of variation is 0.10. By comparing and analysing the calculation results and the Monte-Carlo method, the calculation results are 0.99992 under tension and compression. Both are greater than 0.99999 to meet the reliability requirements.

Table 8
Target reliability of oil and gas pipeline.

Organization	Target reliability			area of application	Limit state
	Low risk	Medium risk	High risk		
GB/T29167-2012	1−0.90	0.90−0.99	0.99−0.999	submarine pipeline	SLS
	$\frac{5\times10^{-3}}{PD^3}$	$\frac{5\times10^{-4}}{PD^3}$	$\frac{5\times10^{-5}}{PD^3}$	Onshore pipeline	SLS
ISO 16708-2006	$1-10^{-3}$	$1-10^{-4}$	$1-10^{-5}$	submarine pipeline	ULS FLS ALS
CSA Z662-2011	0.90	0.90	0.90	Onshore pipeline	SLS
	$1-\frac{1650}{(PD^3)^{0.66}}$	$1-\frac{197}{(\rho PD^3)^{0.66}}$	$1-\frac{49700}{\rho PD^3}$		ULS
	0.99	0.99	0.99		LLS
DNV-OS-F101	0.99	0.999	0.999	submarine pipeline	SLS
	0.9999~	0.99999~	0.999999~		ULS
	0.99999	0.999999	0.9999999		ALS
	0.999	0.9999	0.99999		FLS
API579	0.977	0.999	0.999	Onshore pipeline	SLS
C-FER	$1-10^{-6}$ times/m·year	$1-10^{-7}$ times/m·year	$1-10^{-10}$ times/m·year	Onshore pipeline	SLS ULS

Note: SLS is Serviceabilty Limit State; ULS is Ultimate Limit States; LLS is Leak Limit State; ALS is Accidental Limit States; FLS is Fatigue Limit States.

6.3. Parameter sensitivity analysis

Considering the effects of trench parameters, such as buried depth, pipe diameter, wall thickness, soil characteristics, crossing angle, and fault displacement on the reliability of natural gas pipeline under the action of faults, this paper used a Monte Carlo method to increase the initial standard deviation of each sensitive parameter by 50% each time as new data, sensitivity analysis was conducted four times for each parameter, and the results are displayed in Fig. 19 and Fig. 20. The initial standard deviation of each sensitive parameter is shown in Table 9.

It can be seen from Fig. 19 that when the pipeline is tensioned and the standard deviation increases by 50%, the reliability of pipeline depth, sand friction angle, pipe diameter, and pipeline displacement has begun to decline, which cannot meet the target reliability standards for high-risk areas. With the continuous increase in standard deviation, the effects of pipe diameter and sand friction angle on the reliability are the most significant. When the standard deviation exceeds 100%, the target reliability value of the buried depth and friction angle are slightly lower than the low-risk area reliability standards, which decreases to 0.932174 and 0.974532, respectively.

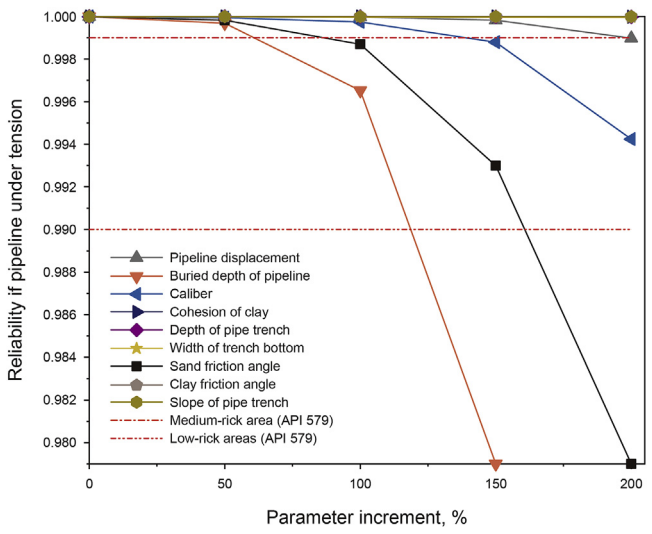

Fig. 19. Sensitive parameter curve of tensile strain.

The sensitivity of each parameter to pipeline reliability from large to small is pipeline buried depth, sand friction angle, pipe diameter, pipeline displacement, width of trench slope bottom, trench depth, clay cohesion, trench slope and clay friction angle.

It can be seen from Fig. 20 that when the pipeline is in compression and the standard deviation increases by 50%, the reliability of various parameters of the pipeline is basically not affected. The reliability values of trench depth and clay cohesion begin to decline when the standard deviation increases to 100%. When the standard deviation is increased to 200%, these values are reduced to 0.999498 and 0.999494, respectively, which can only satisfy the target reliability standards of medium-risk areas, with other parameters being basically unaffected.

When the pipeline is compressed, the changes in clay cohesion and trench depth are more sensitive. However, the other parameters are quite unchanged. The reason is that in the same range of variation, the pipeline compression is more reliable than the pipeline tension by comparing two sets of data of pipeline under tension and compression in Figs. 19 and 20. And with the increase of the standard deviation, the reliability of the parameters in the pipeline tension will continue to decline.

7. Conclusion and prospects

In this study, based on the ABAQUS finite element software, a three-dimensional pipe-soil contact analysis model considering pipe trench parameters is established. In this work, a hundred sets of stochastic simulations were carried out. The conditions for supporting the analysis were verified by 2.2 finite element model validation and 4.2.4 engineering examples. The calculation results of the trench free model under the same working conditions are compared with the calculation results in the ASCE Guide (1984), and the actual strain data of the 40 sets of west east gas transmission pipeline are compared with the calculation results of the model. The three-dimensional pipe-soil contact analysis model provides theoretical support for the calculation of soil spring stiffness of seismic pipeline, which can provide some references to perfect ASCE.

The regression formula of tensile and compressive strain considering the pipe trench parameters is obtained by fitting, and the influence rules of various parameters on pipeline strain are

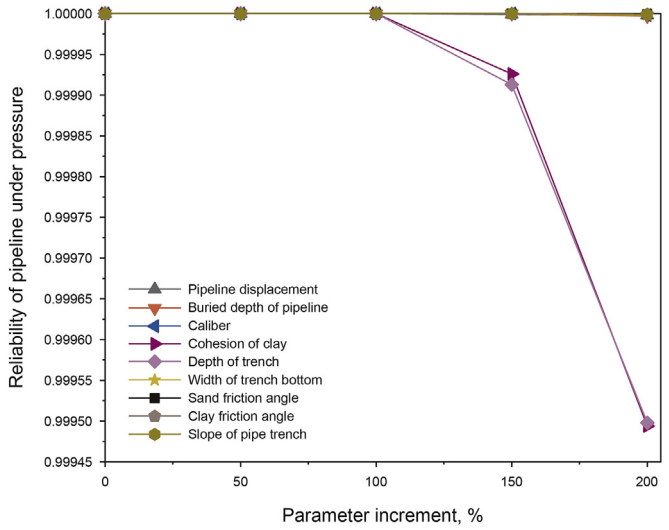

Fig. 20. Sensitive parameter curve of compressive strain.

Table 9
Initial standard deviation of each sensitive parameter.

Sensitive parameter	Initial standard deviation
Pipeline displacement	0.04
Buried depth	0.15
Diameter	0.10
Cohesion of clay	4
Trench depth	0.23
Bottom width	0.30
Sand friction angle	0.03
Clay friction angle	0.04
Trench slope	0.06

summarized as follows. Because of reducing the complexity of the simulation, these equations are suitable for engineering projects. This study can provide reference for the aseismic design of buried pipelines, and provide protection for the safe operation of pipelines.

(1) The failure location of the pipeline, that is, the extreme strain is mainly located within 2.50 m on both sides of the fault center. The compressive strain is more sensitive to the crossing angle and the larger crossing angle can effectively reduce the maximum values of axial displacement and axial compressive strain of pipeline. The tensile deformation and failure of the cross-fault pipeline are the main manifestations under the influence of a large amount of dislocation. The mechanical parameters of the cross-fault pipeline can be effectively reduced when the fault crack width is large.
(2) The reliability of pipeline in China 2nd west-east gas pipeline project is 0.99992 under tension and compression, both of which are greater than 0.99999, meeting the reliability requirements.
(3) When the pipeline is in tension and the standard deviation increases by 50%, the buried depth, sand friction angle, pipe diameter and pipeline displacement can not meet the target reliability standard of high-risk area. With the increase of standard deviation, pipe diameter and sand friction angle have the greatest impact on the reliability. When the standard deviation changes more than 100%, the target reliability values of pipeline buried depth and sand friction angle are lower than the standard of low risk area one by one. When the standard deviation increases by 50%, the reliability of each parameter of the pipeline basically has no influence. When the standard deviation changes to 100%, the reliability value of pipe trench depth and clay cohesion begins to decline. When the standard deviation reaches 200%, the depth of pipe trench and clay cohesion decrease to 0.999498 and 0.999494 respectively, which can only meet the target reliability standard in medium risk areas, and other parameters are not affected Ring.
(4) The sensitivity of each parameter to pipeline reliability from large to small is pipeline buried depth, sand friction angle, pipe diameter, pipeline displacement, width of trench slope bottom, trench depth, clay cohesion, trench slope and clay friction angle; when the pipeline is under pressure, the influence of trench depth and clay cohesion is greater, and other parameters have less influence.

The seismic limit state equation of natural gas pipeline based on strain was constructed using the fitting method. The error analysis of the fitting formula was carried out, and the accuracy of the equation was verified by combining the actual working condition data. Based on the results of this study, the authors hope to continue to improve and carry out the following investigations in future research:

(1) It is planned to construct limit state equations of various fault types, including normal fault, strike-slip fault, and composite fault, to make the equations universal.
(2) Because of the complexity of the fitting formula considering the parameters of the pipe trench, the next step is to optimise and adjust the fitting formula so that it can be applied in practice.

Acknowledgements

The authors acknowledge the financial support by China Petroleum Science & Technology Innovation Fund (2017D-5007-0606): Reliability research of large diameter and high steel natural gas pipeline under fault action.

References

Cheng, X.D., Ma, C., Huang, R.K., Yang, W.D., 2019. Failure mode analysis of X80 buried steel pipeline under oblique-reverse fault. Soil Dynam. Earthq. Eng. 125 (Oct). https://doi.org/10.1016/j.soildyn.2019.105723, 105723.1-105723.11.
Cheng, X.D., Pang, M.W., Xu, L., Su, Q.Z., Xiang, E.Z., Hu, W.J., 2016. Seismic response analysis of bu-ried pipeline crossing inclined slip fault based on strain design. Nat. Gas. Ind. 36 (10), 110–117. https://doi.org/10.3787/j.issn.1000-0976.2016.10.014 (in Chinese).
Chen, C., Xi, Z.D., Zhu, W.H., 2013. A new method to assess the structural reliability of gas pipelines containing defects, 06 Oil Gas Storage Transp. 32, 590–593. https://doi.org/10.6047/j.issn.1000-8241.2013.06.005 (in Chinese).
Fan, H., Xie, X.F., X, Y., Lv, X.F., Yan, X.Z., 2016. Seismic reliability evaluation method of long distance pipeline based on strain design. Sci. Technol. Eng. 16 (23), 181–184. https://doi.org/10.3969/j.issn.1671-1815.2016.23.034 (in Chinese).
Gu, X.T., Zhang, H., 2009. Research on aseismatic measures of gas pipeline crossing a fault for strain-based design. In: 2009 ASME Pressure Vessels and Piping Division Conference. https://doi.org/10.1115/PVP2009-77987, 26-30 July, Prague, Czech Republic.
Hassanien, S., Leblanc, L., Nemeth, A., 2016. Towards an acceptable pipeline integrity target reliability. In: Proceedings of the 2016 11th International Pipeline Conference. https://doi.org/10.1115/ipc2016-64425, 26-30 September, Calgary, Alberta.
Joshi, S., Prashant, A., Deb, A., Jain, S.K., 2011. Analysis of buried pipelines subjected to reverse fault motion. Soil Dynam. Earthq. Eng. 31 (7), 930–940. https://doi.org/10.1016/j.soildyn.2011.02.003.
Jalali, H.H., Rofooei, F.R., Attari, N.K.-A., Samadian, M., 2016. Experimental and finite element study of the reverse faulting effects on buried continuous steel gas pipelines. Soil Dynam. Earthq. Eng. 1–14. https://doi.org/10.1016/j.soildyn.2016.04.006, 86(Jul.).
Karamitros, D.K., Bouckovalas, G.D., Kouretzis, G.P., 2007. Stress analysis of buried steel pipelines at strike-slip fault crossings. Soil Dynam. Earthq. Eng. 27 (3), 200–211. https://doi.org/10.1016/j.soildyn.2006.08.001.

Karamitros, D.K., Bouckovalas, G.D., Kouretzis, G.P., Gkesouli, V., 2011. An analytical method for strength verification of buried steel pipelines at normal fault crossings. Soil Dynam. Earthq. Eng. 31 (11), 1452–1464. https://doi.org/10.1016/j.soildyn.2011.05.012.

Kennedy, R.P., Inc, Irvine, Chow, A.W., Williamson, R.A., 1977. Fault movement effects on buri-ed oil pipeline. J. Transport. Eng. 103 (5), 617–633. https://doi.org/10.1007/BF00148804.

Liu, X.B., Chen, Y.F., Zhang, H., Xia, M.Y., Zheng, W., Zhang, Z.Y., Liang, L.C., Chen, J.X., 2014. Prediction on the design strain of the X80 steel pipelines across active faults under stress. Nat. Gas. Ind. 34 (12), 123–130. https://doi.org/10.3787/j.issn.1000-0976.2014.12.018 (in Chinese).

Li, Q.C., He, S., 2021. Research on effect factors of mechanical response of cross-fault buried gas pipeline based on fluid-structure interaction. J. Pressure Vessel Technol. 143 (6), 061402. https://doi.org/10.1115/1.4051366.

Li, X.J., Shen, F.M., 2015. Seismic connectivity reliability analysis of urban water supply network at different earthquake intensities. J. Chongqing Univ. 38 (6), 123–128. https://doi.org/10.11835/j.issn.1000-582X.2015.06.017 (in Chinese).

Li, P., Tao, Y.L., Zhou, J., 2013. A study of the ultimate compressive strain of local buckling in strain-based design of pipelines. Nat. Gas. Ind. 33 (7), 101–107. https://doi.org/10.3787/j.issn.1000-0976.2013.07.018 (in Chinese).

Liu, M., Wang, Y.Y., Yu, Z.F., 2008. Response of pipelines under fault crossing. In: The Proceedings of the Eighteenth International Offshore and Polar Engineering Conference, 6 July, Vancouver, Canada.

Li, Y., Yu, J.X., Yu, Y., Han, M.X., Li, M.Z., Yu, J.H., 2019. Research on local buckling and strain response prediction of submarine pipelines across strike-slip faults, 04 World Earthq. Eng. 35, 105–113 (in Chinese).

Liu, X.B., Zhang, H., Gu, X.T., Chen, Y.F., Xia, M.Y., Wu, K., 2017. Strain demand prediction method for buried X80 steel pipelines crossing oblique-reverse faults. Earthqu. Struct. 12 (3), 321–332. https://doi.org/10.12989/eas.2017.12.3.321.

Liu, X.B., Zheng, Q., Wu, K., Yang, Y., Zhao, Z.Q., Zhang, H., 2020. Development of a novel approach for strain demand prediction of pipes at fault crossings on the basis of multi-layer neural network driven by strain data. Eng. Struct. 214 (Jul.1). https://doi.org/10.1016/j.engstruct.2020.110685, 110685.1-110685.9.

Newmark, N.M., Hall, W.J., 1975. Pipeline design to resist large fault displacement. In: Proceedings of US National Conference on Earthquake Engineering, 18-20 March, Ann Arbor, Michigan.

Trifonov, O.V., Cherniy, V.P., 2010. A semi-analytical approach to a nonlinear stress–strain analysis of buried steel pipelines crossing active faults. Soil Dynam. Earthq. Eng. 30 (11), 1298–1308. https://doi.org/10.1016/j.soildyn.2010.06.002.

Tao, K.E., Sun, Y.W., 2015. Analysis of Seismic Reliability for Buried Pipelines Crossing Fault, vol. 9. Northeast Petroleum University, pp. 1–4. https://doi.org/10.19537/j.cnki.2096-2789.2017.09.001 (in Chinese).

Vasileios, E.M., Dimitrios, V., Charis, J.G., 2014. Seismic risk assessment of buri-ed pipelines at active fault crossings. In: Second European Conference on Earthquake Engineering and Seismology. https://doi.org/10.1193/122015EQS187M, 25–29 August, Istanbul.

Wang, G.L., Han, J.K., Zhao, Z.D., Ma, W.G., Du, X.J., Zhao, L.J., 2011. Application of the strain to the pipeline construction. Petrol. Plan. Eng. 22 (5), 1–6 https://doi.org/CNKI:SUN:SYGH.0.2011-05-003 (in Chinese).

Wei, X.L., Jiao, W.S., Zeng, X., Zhang, D.F., Du, G.F., Vignali, V., 2021. Mechanical behavior of buried pipelines subjected to faults. Adv. Civ. Eng. 2021 (3), 1–19. https://doi.org/10.1155/2021/9984519.

Wisianto, A., Kodiyat, H., 2003. Managing safety and reliability of a submarine gas pipeline: east java gas pipeline case study. In: Twenty-Ninth Annual Convention and Exhibition. https://doi.org/10.29118/ipa.1051.03.b.008, 1 October, Indonesian.

Wang, L.J., Wang, L.R.L., 1995. Buried pipelines in large fault movements. In: 4. U.S. Conference on Lifeline Earthquake Engineering, 10-12 August, San Francisco United states.

Wang, R.L., Yeh, Y.H., 1985. A refined seismic analysis and design of buried pipeline for fault movement. Earthq. Eng. Strut. Dyn. 13 (1), 75–96. https://doi.org/10.1002/eqe.4290130109.

Yu, Z.F., Shi, H., Tong, L., Liu, R., 2010. Application of strain-based design method in west-to-east parallel gas transmission pipeline project. Oil Gas Storage Transp. 29 (2), 143–147 https://doi.org/CNKI:SUN:YQCY.0.2010-02-020 (in Chinese).

Yu, W.C., Wen, K., Min, Y., He, L., Huang, W.H., 2018. A methodology to quantify the gas supply capacity of natural gas transmission pipeline system using reliability theory. Reliab. Eng. Syst. Saf. 175 (Jul.), 128–141. https://doi.org/10.1016/j.ress.2018.03.007.

Zhang, J., Chen, Y., Liang, B.F., Pan, B., 2021. Damage evolution mechanism of buried pipeline crossing reverse fault. J. Mech. Sci. Technol. 35 (1), 71–77. https://doi.org/10.1007/s12206-020-1206-0.

Zhang, X.Y., Feng, J., 2013. Oil and gas pipeline residual strength research based on reliability analysis. Appl. Mech. Mater. 2400 (636), 562–566. https://doi.org/10.4028/www.scientific.net/amm.318.562.

Zhao, X.W., Zhang, H., Luo, J.H., 2016. Risk acceptance criteria for oil and gas pipelines. Oil Gas Storage Transp. 35 (1), 1–6. https://doi.org/10.6047/j.issn.1000-8241.2016.01.001 (in Chinese).

Zheng, Q., Zhang, H., Liu, X.B., 2020. Reliability analysis of pipeline in fault area based on BP-MC method. Oil Gas Storage Transp. 29 (3), 277–283. https://doi.org/10.6047/j.issn.1000-8241.2020.03.004 (in Chinese).

Zhang, J.Y., Zhang, Z.Y., Yu, Z.F., Wu, W., 2014. Building a target reliability adaptive to China onshore natural gas pipeline. In: Proceedings of the 2014 10th International Pipeline Conference. https://doi.org/10.1115/IPC2014-33129. September 29 - October 3, Calgary, Alberta, Canada.

Zhang, Z.Y., Zhou, Y.W., Zhang, J.Y., 2016. Assessment on design factors of China's natural gas P-ipeline based on reliability-based design method. In: Proceedings of the 2016 11th International Pipeline Conference. https://doi.org/10.1115/ipc2016-64186, 26-30 September, Calgary, Alberta.